Electronic Supplementary Material (ESI) for Journal of Materials Chemistry A.

Supporting Information

for

Poly(NIPAM-*co*-thienoviologen) for Multi-responsive Smart Windows and Thermo-controlled Photodynamic Antimicrobial Therapy

Yueyan Zhang,[a] Kun Zhou,[a] Huaiyu Jiang,[b] Suikun Zhang,[a] Bingjie Zhang,[a] Mengying Guo,[a] and Gang He [a,c]*

[a]Frontier Institute of Science and Technology, State Key Laboratory for Strength and Vibration of Mechanical Structures, Key Laboratory of Shaanxi Province for Craniofacial Precision Medicine Research College of Stomatology, Xi'an Jiaotong University, Xi'an, Shaanxi 710054, China

[b]Xi'an Jiaotong University Health Science Center, Xi'an, Shaanxi 710054, China

[c]Guangdong Provincial Key Laboratory of Functional and Intelligent Hybrid Materials and Devices, South China University of Technology, Guangzhou 510640, China

*Email: ganghe@mail.xjtu.edu.cn.

Table of Contents

1. Materials and Instrumentation

Materials. All reactions were performed with standard Schlenk and glovebox (Vigor) techniques under inert atmosphere. 2,5-Dibromothiophene (98%), 5,5'-Dibromo-2,2'-bithiophene (98%), 2,2':5',2"-Terthiophene (97%), methyltrioctylammonium chloride (Aliquant 336, 98%), and tetrakis(triphenylphosphine)palladium(0) (Pd (PPh_3)$_4$), 99%) N-isopropylacrylamide (NIPAM, 98%, stabilized with MEHQ), ammonium persulfate (APS, 99%) and N,N,N',N'-tetramethylethylenediamine (TEMED, 99%) were perched from Energy Chemical Inc. and used as received. Toluene was distilled from sodium-benzophenone system before use. Other solvents were purchased and used without any further purification.

NMR spectra were recorded on a Bruker Avance-400 spectrometer in the indicated solvents. Chemical shifts are reported in ppm by assigning TMS resonance in the ^{1}H spectra as 0.00 ppm, DMSO-d_6 resonance in the ^{13}C spectra as 39.50 ppm. Coupling constants are reported in Hz and multiplicities were denoted as s (singlet), d (doublet), t (triplet), q (quartet) and m (multiplet). UV-Vis spectra were measured using a DH-2000-BAL Scan spectrophotometer. The cyclic voltammetry (CV) in solution were measured using CHI660E B157216, with a polished glassy carbon electrode as the working electrode, a platinum electrode as the counter electrode, and silver electrode as the reference electrode, using ferrocene/ferrocenium (Fc/Fc^+) as internal standard. The molecular weight of the polymers was measured by gel permeation chromatography (GPC) equipped with an isocratic pump (waters 2414), a DAWN HELEOS 18-angle laser light scattering detector (Wyatt Technology, Santa Barbara, CA), and an Optilab rEX refractive index detector (Wyatt Technology, Santa Barbara, CA). Separations were achieved using size-exclusion columns connected in series (400, 103, and 104 Å Phenogel columns, 5 μm, 300 × 7.8 mm, Phenomenex, Torrance, CA) utilizing DMF containing 0.1 M LiBr as the mobile phase at a flow rate of 1.0 mL min^{-1}. The concentration of polymer was 1~2 mg/mL. Monodisperse polystyrene was used as the standard. Thermogravimetric analysis (TGA) measurements were conducted using of a Mettler-Toledo TGA1 thermal analyser in air, at a heating rate of 10 °C min^{-1} in the temperature range of 30-700 °C. Differential scanning calorimetry (DSC) was utilized to determine the thermal transition properties using a DISCOVER DSC250 (TA instruments) in a temperature range of -50 °C to 200 °C with a ramp rate of 10 °C min^{-1} under an inert atmosphere. The heating and cooling cycles were repeated three times. High-resolution mass spectra (HRMS) were recorded on a Bruker maxis UHR-TOF mass spectrometer in an ESI positive mode. Fluorescence measurements were performed on FLS920 system (Edinburgh Instruments). Fourier transform infrared spectroscopy (FTIR) was collected with Nicolet 6700 FT-IR Instrument. Melting points were determined with an SGW X-4 microscopic melting point apparatus. EPR was measured using a Bruker EMX PLUS6/1 instrument at room temperature in dry degassed DMF. Malvern Zetasizer Nano ZSE was used to measure the Zeta potential of bacteria before and after addition of photosensitizers. KRUSS Drop Shape Analyzer-DSA100S was used to measure the water contact angle of polymer films. In the solution-based ECD, Indium tin oxide (ITO)-coated

glass was utilized as the electrodes and polymer **4a**-**4c** was used as active component. The two slides of ITO glass were stick together with a UV-cured gasket with 50 μm-thick intervals introduced by Baumgartner group. Bacterial killing assay processed under visible light through a Mejiro Genossen MVL-210 photoreactor. Photographs were taken with a Nikon D5100 digital camera.

2. Experimental conditions

Step 1: Synthesis of thienobipyridine

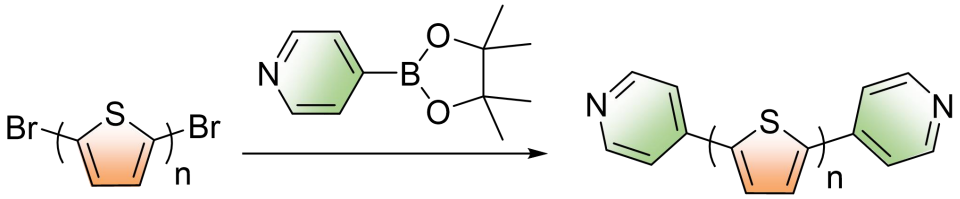

1a-1c **2a-2c**

n = 1, 2, 3

Scheme S1. Synthetic routes to **2a-2c**.

Dibromo-thiophene derivatives 1a-1c were purchased or synthesized *via* reported procedures.[1] **1** (4.1 mmol), 4-Pyridineboronic acid pinacol ester (12.4 mmol), $Pd(PPh_3)_4$ (0.2 mmol), methyltrioctylammonium chloride (Aliquant 336, 5 drops) was added to a schlenk flask and degassed. Degassed K_2CO_3 aqueous solution (2.0 M, 18.6 mL) was added under Ar protection. The reaction mixture was stirred at reflux overnight. After remove the solvent by rotovap, the crude product was extracted with chloroform. HCl (aq) was added until precipitation was formed. The precipitate was filtered and dissolved in water. 15 M NaOH (aq) was added until the pH of the system reaches 8~9. The obtained precipitate was filtered as final product.

Thienobipyridine **2a**

^{1}H NMR (400 MHz, DMSO-d_6): δ 8.63 (dd, *J* = 6.4 Hz, 4H, PyH), 7.93 (s, 2H, TH), 7.72 (dd, *J* = 6.4 Hz, 4H, PyH). ^{13}C NMR (100 MHz, DMSO-d_6): δ 150.56, 141.74, 139.88, 128.11, 119.51. HRMS (ESI) m/z: calcd for $[C_{14}H_{10}N_2S + H^+]^+$ 239.0637; found 239.0632; UV/vis (in DMF): λ_{max} (***ε***) = 334 nm (4.046×10^4 M^{-1} cm^{-1}); Fluorescence emission (in DMF) (λ_{ex} = 339 nm): λ_{emis} = 386 nm; mp (°C): > 300.

Dithienobipyridine **2b**

^{1}H NMR (400 MHz, DMSO-d_6): δ 8.60 (d, *J* = 5.6 Hz, 4H, PyH), 7.86 (d, *J* = 4 Hz, 2H, TH), 7.68 (d, *J* = 5.6 Hz, 4H, PyH), 7.55 (d, *J* = 4 Hz, 2H, TH). ^{13}C NMR (100 MHz, DMSO-d_6): δ 150.49, 139.87, 139.65, 137.44, 127.95, 126.38, 119.30. HRMS (ESI) m/z: calcd for $[C_{18}H_{12}N_2S_2 + H^+]^+$ 321.0515; found 321.0512; UV/vis (in DMF): λ_{max} (ε) = 385 nm (5.066×10^4 M^{-1} cm^{-1}); Fluorescence emission (in DMF) (λ_{ex} = 396 nm): λ_{emis} = 454 nm; mp (°C): > 300.

Terthienobipyridine **2c**

^{1}H NMR (400 MHz, $CDCl_3$): δ 8.61 (d, *J* = 5.6 Hz, 4H, PyH), 7.47 (d, *J* = 6 Hz, 4H, PyH), 7.46 (d, *J* = 4 Hz, 2H, TH), 7.22 (d, *J* = 4 Hz, 2H, TH), 7.19 (s, 2H, TH). ^{13}C NMR (100 MHz, DMSO-d6): δ

150.55, 141.02, 140.02, 138.72, 136.42, 126.44, 125.31, 125.12, 119.62. HRMS (ESI) m/z: $[C_{22}H_{14}N_2S_3 + H^+]^+$ calcd for 403.0392; found 403.0386; UV/vis (in H_2O): λ_{max} (ε) = 416 nm (5.372×10^4 M^{-1} cm^{-1}); Fluorescence emission (in DMF) (λ_{ex} = 419 nm): λ_{emis} = 476 nm; mp (°C): > 300.

Step 2: Synthesis of thienoviologens

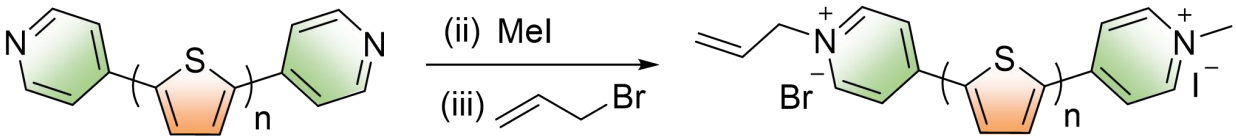

2a-2c **3a-3c**

Scheme S2. Synthetic routes to thiophene-extended viologens **3a-3c**.

2 (0.15 mmol) was added to a schlenk flask and degassed. Iodomethane (0.18 mmol, 1.2 eq) and methyl nitrite (5 mL) was added. The reaction mixture was heated at 60 °C for 2 h. Allyl bromide (0.18 mmol, 1.2 eq) was added and the reaction mixture was heated at 60 °C for 2 h. The product was filtered and washed with DCM.

Thienoviologen **3a**

^{1}H NMR (400 MHz, DMSO-d_6) δ 9.04 (dd, *J* = 17.8, 6.2 Hz, 4H), 8.49 (m, 6H), 6.19 (m, 1H), 5.47 (d, *J* = 10.3 Hz, 1H), 5.42 (d, *J* = 17.2 Hz, 1H), 5.03 (d, *J* = 6.3 Hz, 2H), 4.33 (s, 3H) ppm. ^{13}C NMR (100 MHz, **3c** in D_2O) δ 146.52, 145.72 142.86, 134.28, 134.00, 132.2, 123.78, 123.28, 122.24, 62.19, 47.77 ppm. HRMS (ESI) m/z: calcd for [M-I^--Br^-] $C_{18}H_{28}N_2S^{2+}$ 147.0590; found 147.0591; UV/vis (in H_2O): λ_{max} (ε) = 380 nm (3.570×10^4 M^{-1} cm^{-1}); Fluorescence emission (in H_2O) (λ_{ex} = 330 nm): λ_{emis} = 426 nm; mp (°C): > 300

Bithienoviologen **3b**

^{1}H NMR (400 MHz, D_2O) δ 8.56 (dd, *J* = 21.1, 6.6 Hz, 4H), 8.08 (dd, *J* = 12.6, 6.6 Hz, 3H), 7.92 (dd, *J* = 7.6, 4.2 Hz, 2H), 7.56 (s, 2H), 6.22 – 5.86 (m, 1H), 5.46 (d, J = 10.3 Hz, 1H), 5.37 (d, *J* = 17.1 Hz, 1H), 5.03 (d, *J* = 6.3 Hz, 2H), 4.19 (s, 3H) ppm. ^{13}C NMR (100 MHz, D_2O) δ 147.79, 147.11, 146.10, 145.30, 142.34, 142.99, 142.00, 141.94, 137.75, 137.68, 137.60, 134.36, 134.01, 132.33, 129.24, 129.09, 122.97, 122.49, 61.85, 47.46 ppm. HRMS (ESI) m/z: calcd for [M-I^--Br^-]$^{2+}$ $C_{22}H_{20}N_2S_2^{2+}$ 188.0528; found 188.0529; UV/vis (in H_2O): λ_{max} (ε) = 412 nm (4.175×10^4 M^{-1} cm^{-1}); Fluorescence emission (in H_2O) (λ_{ex} = 360 nm): λ_{emis} = 505 nm; mp (°C): > 300

Terthienoviologen **3c**

^{1}H NMR (400 MHz, D_2O) δ 8.42 (dd, J = 24.8, 6.6 Hz, 4H), 7.93 (dd, J = 12.1, 6.5 Hz, 4H), 7.77 (dd, J = 10.4, 4.1 Hz, 2H), 7.37 – 7.11 (m, 4H), 6.08 – 5.87 (m, 1H), 5.42 (d, J = 10.3 Hz, 1H), 5.33 (d, J = 17.2 Hz, 1H), 4.89 (d, J = 6.3 Hz, 2H), 4.04 (s, 3H) ppm. ^{13}C NMR (100 MHz, D_2O) δ 147.95, 147.27, 145.96, 145.15, 142.92, 136.44, 135.46, 134.42, 132.36, 128.56, 127.86, 122.64, 122.16,

121.93, 61.78, 47.35 ppm. HRMS (ESI) m/z: calcd for $[M\text{-}I^{-}\text{-}Br^{-}]^{2+}$ $C_{26}H_{22}N_2S_3^{2+}$ 229.0467; found 229.0466; UV/vis (in H_2O): λ_{max} (ε) = 430 nm (5.323 × 10^4 M^{-1} cm^{-1}); Fluorescence emission (in H_2O) (λ_{ex} = 430 nm): λ_{emis} = 572 nm; mp (°C): > 300.

Step 3: Synthesis of multi-responsive viologen polymers **4a-4c**

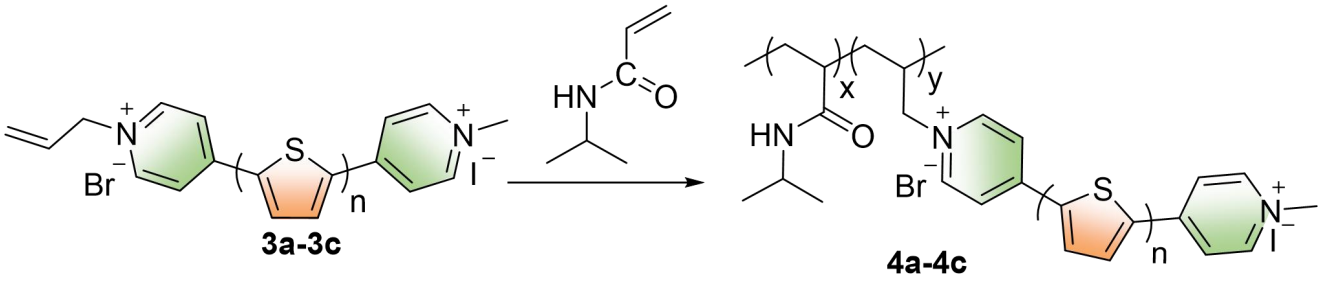

Scheme S3. Synthetic routes to NIPAM-viologen copolymer **4a-4c**.

A precursor mixture containing NIPAM (0.3 g, 2.65 mmol) and AMDPT (10 wt% of NIPAM), ammonium persulfate (1 wt%, initiator) and tetramethylethylenediamine (TEMED) (1 wt%, accelerator) was stirred in H_2O. The mixture was degassed with Ar and reacted at 20 °C for 24 h.

Reactive oxygen species (ROS) measurements

2, 7-dichlorofluorescein diacetate (DCFH-DA) was used to probe the generation of ROS. Under alkaline conditions, DCFH-DA was converted into 2,7-dichlorofluorescin (DCFH), which was followed by transforming into highly fluorescent 2,7-dichloro fluorescein (DCF, excitation 488nm, emission at 525 nm, quantum yield: 90 %) in the presence of ROS. Copolymers were added into the solutions of activated DCFH (40 μM), respectively (The final concentration is 1 μM). The solutions were irradiated under white light (5 mW/cm^2) for 5 min, and emission intensity of DCF solution at 525 nm was recorded every minute with the excitation wavelength of 488 nm.

***In vitro* antibacterial experiments**

The copolymer **4a-4c** were dissolved in MeOH and drop-cast on 1 cm-diameter glass plates and the solvent was evaporated at room temperature. The cell suspension was dropped on the polymer-coated plates and the mixture were exposed to 90 mW/cm^2 white light for 5 min at room temperature or on a hot plate heated to 35 ºC. And then the mixture on the plate was spread on the solid LB agar plate, and the colonies formed after 16 h incubation at 37 ºC were counted. The inhibition ratio was determined by dividing the number of colony-forming unite (CFU). The inhibition ratio (IR) was calculated according to the following equation:

$$\mathrm{IR} = \frac{(C_0 - C)}{C_0} \times 100\%$$

Where C is the CFU of the experimental group treated with compounds, and C_0 is the CFU of the control group without any treatment.

3. NMR spectra

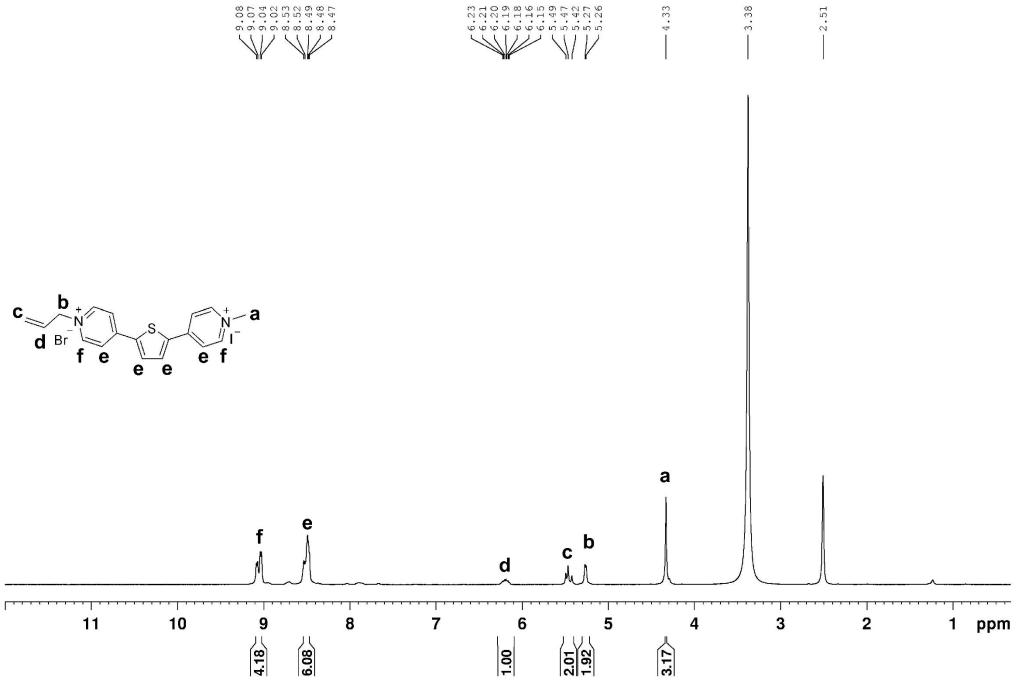

Figure S1. ^{1}H NMR spectrum for **3a** in DMSO-d_6.

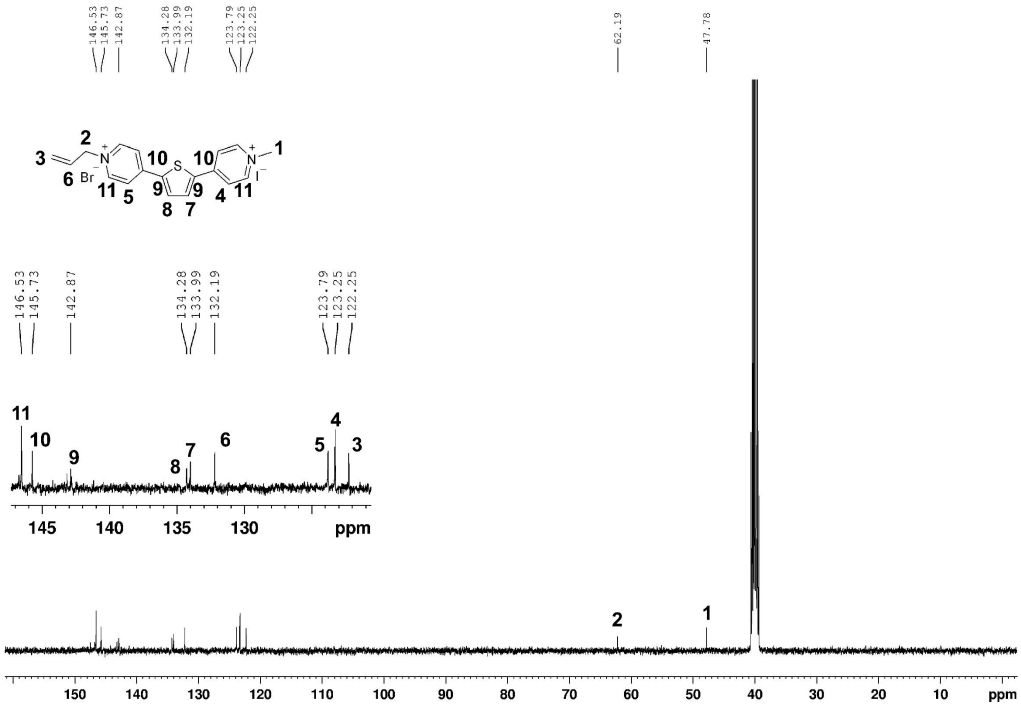

Figure S2. ^{13}C NMR spectrum for **3a** in DMSO-d_6.

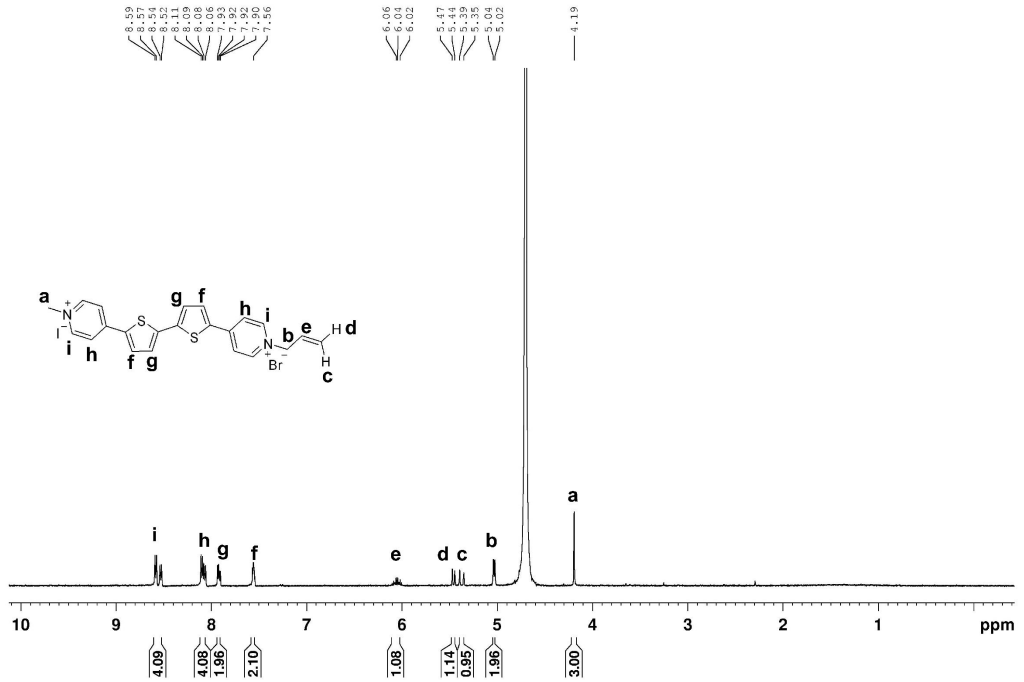

Figure S3. ^{1}H NMR spectrum for **3b** in D_2O.

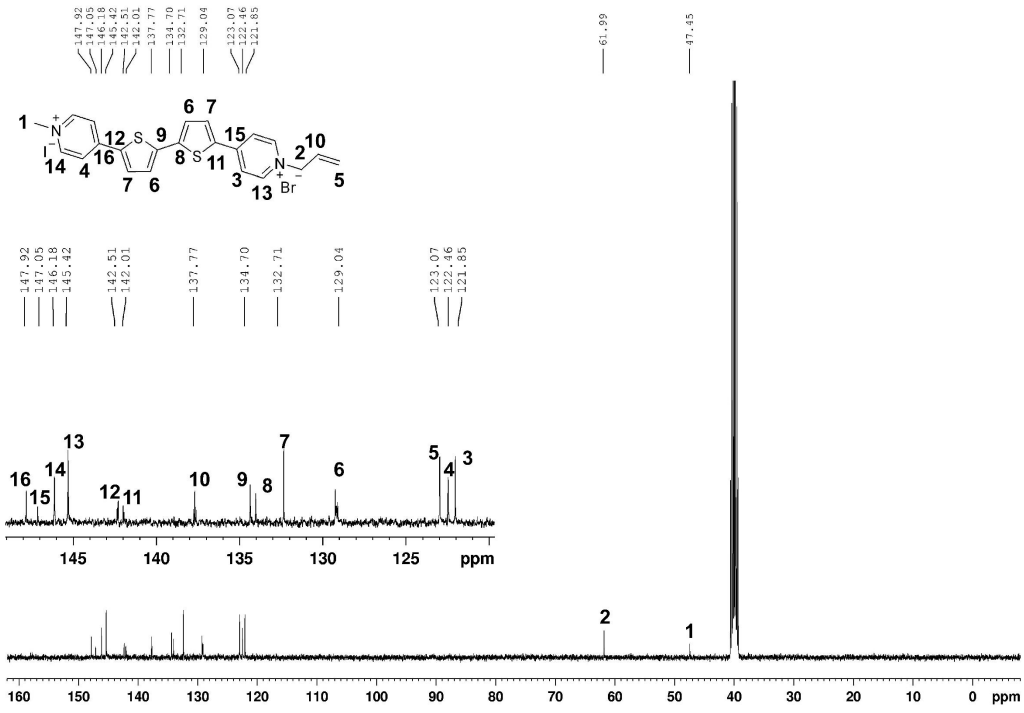

Figure S4. ^{13}C NMR spectrum for **3b** in DMSO-d_6.

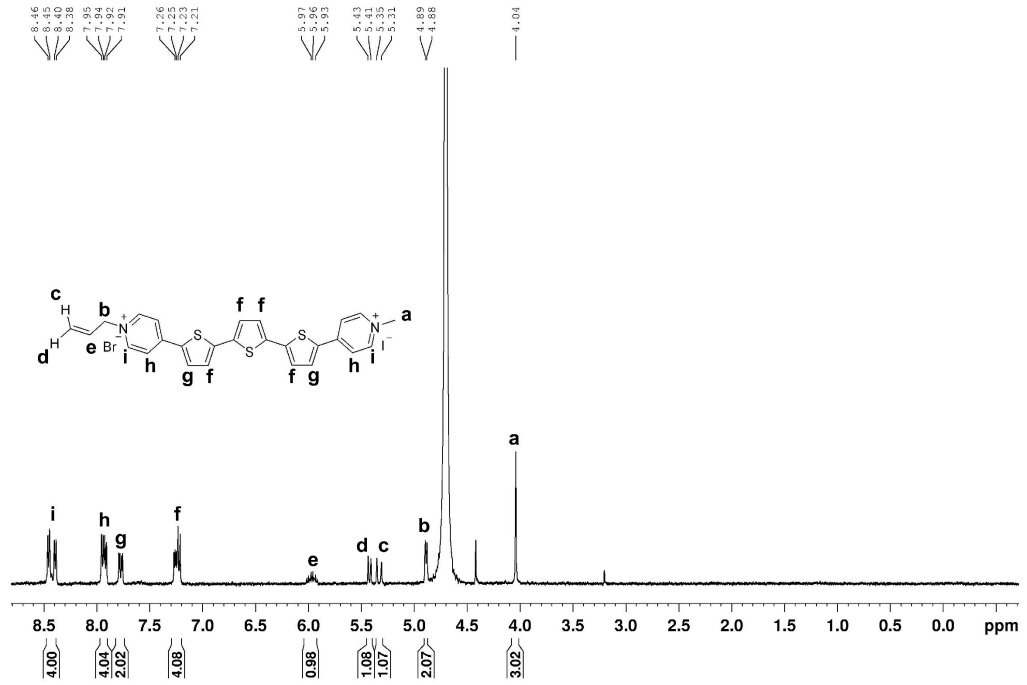

Figure S5. ^{1}H NMR spectrum for **3c** in D_2O.

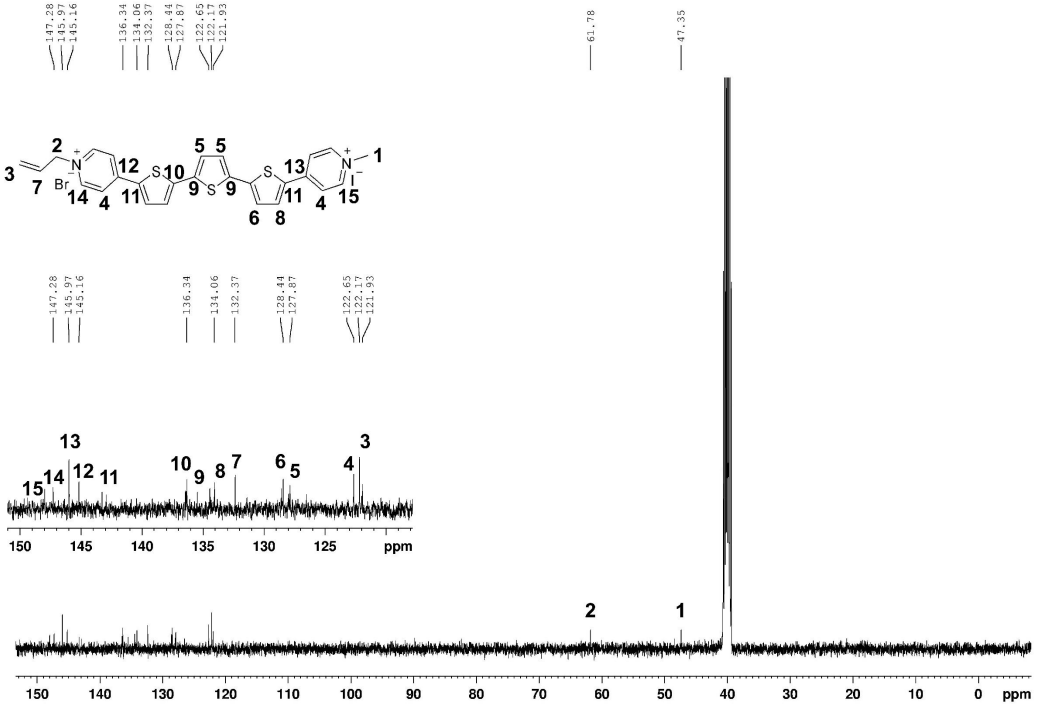

Figure S6. ^{13}C NMR spectrum for **3c** in DMSO-d_6.

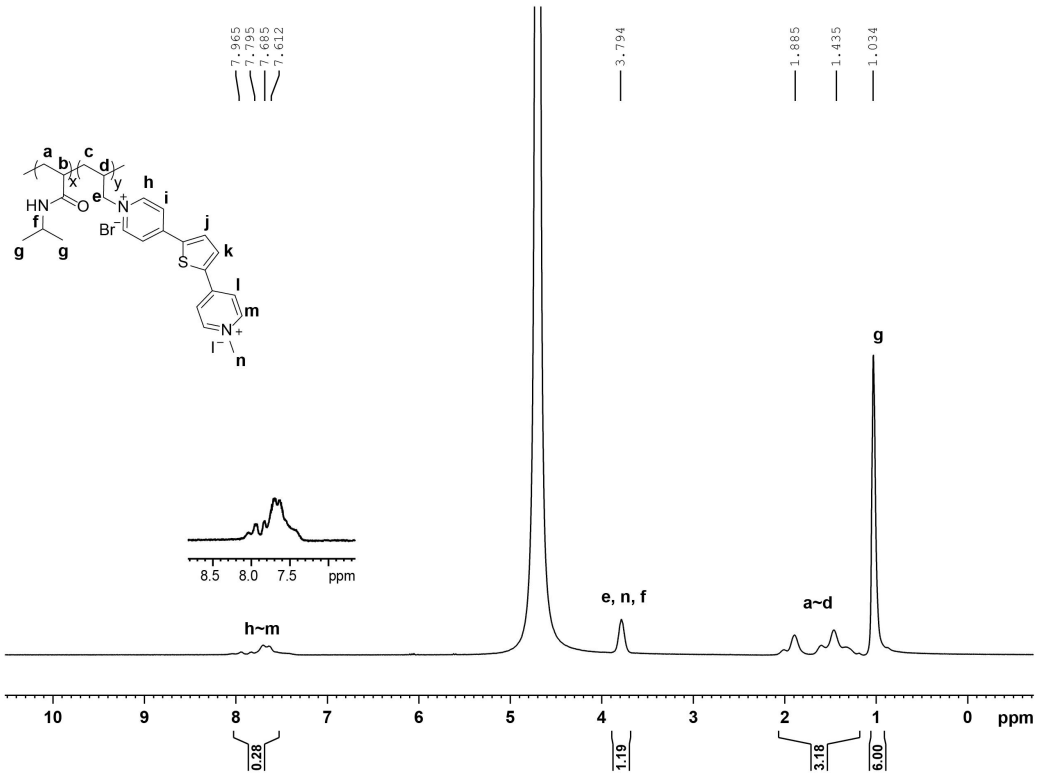

Figure S7. ^{1}H NMR spectrum for **4a** in D_2O.

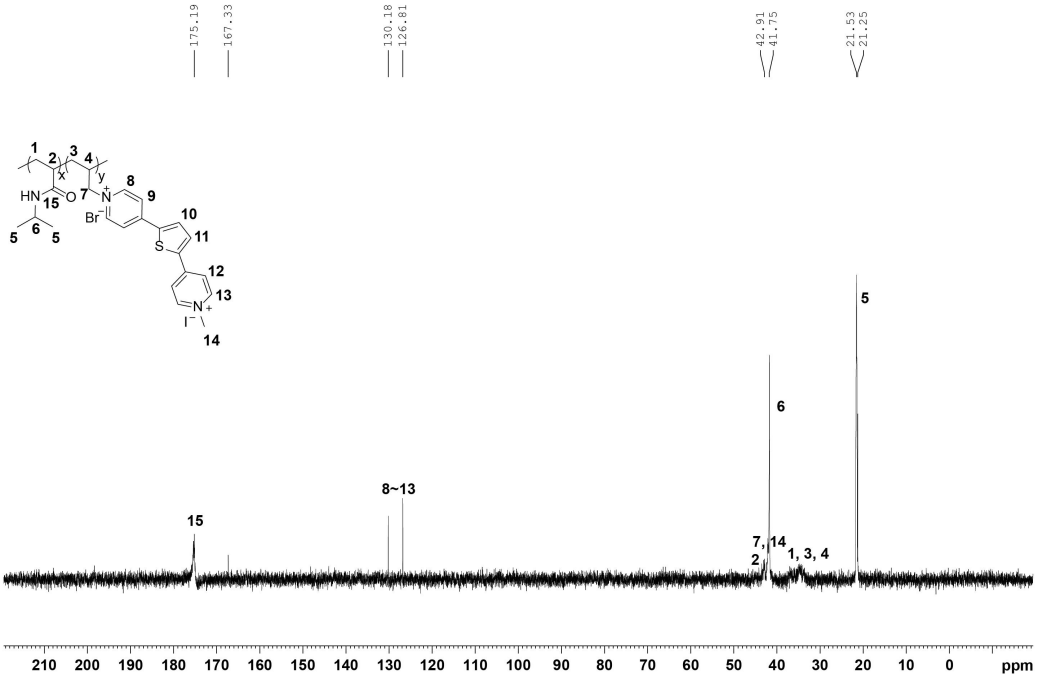

Figure S8. ^{13}C NMR spectrum for **4a** in D_2O.

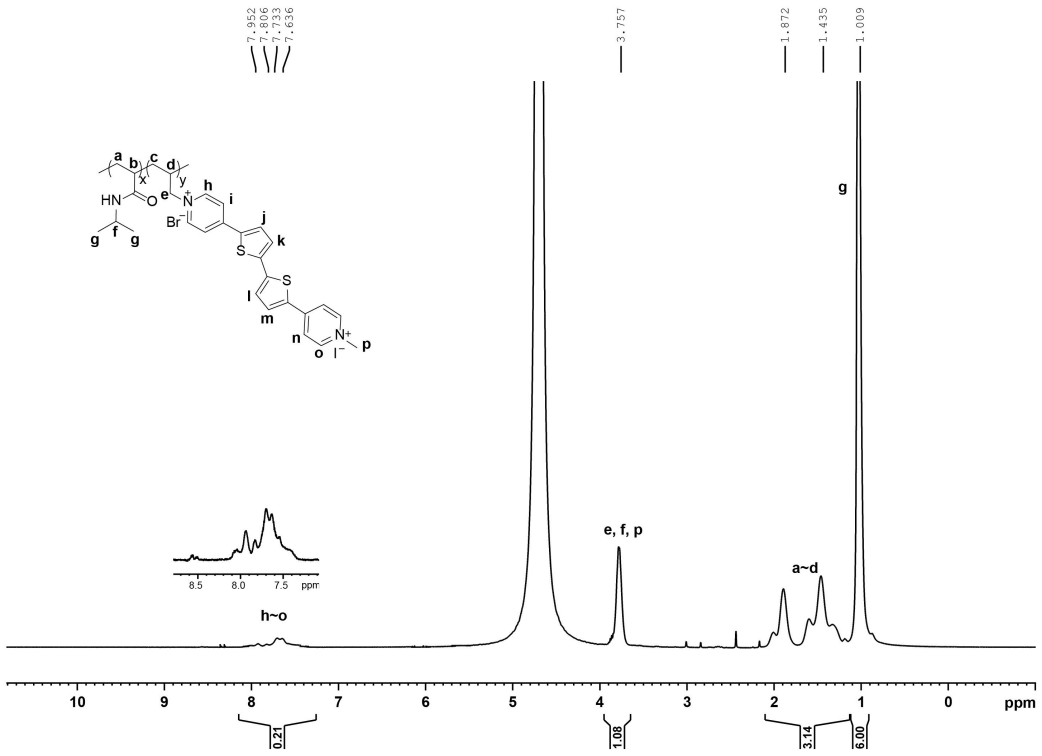

Figure S9. ^{1}H NMR spectrum for **4b** in D_2O.

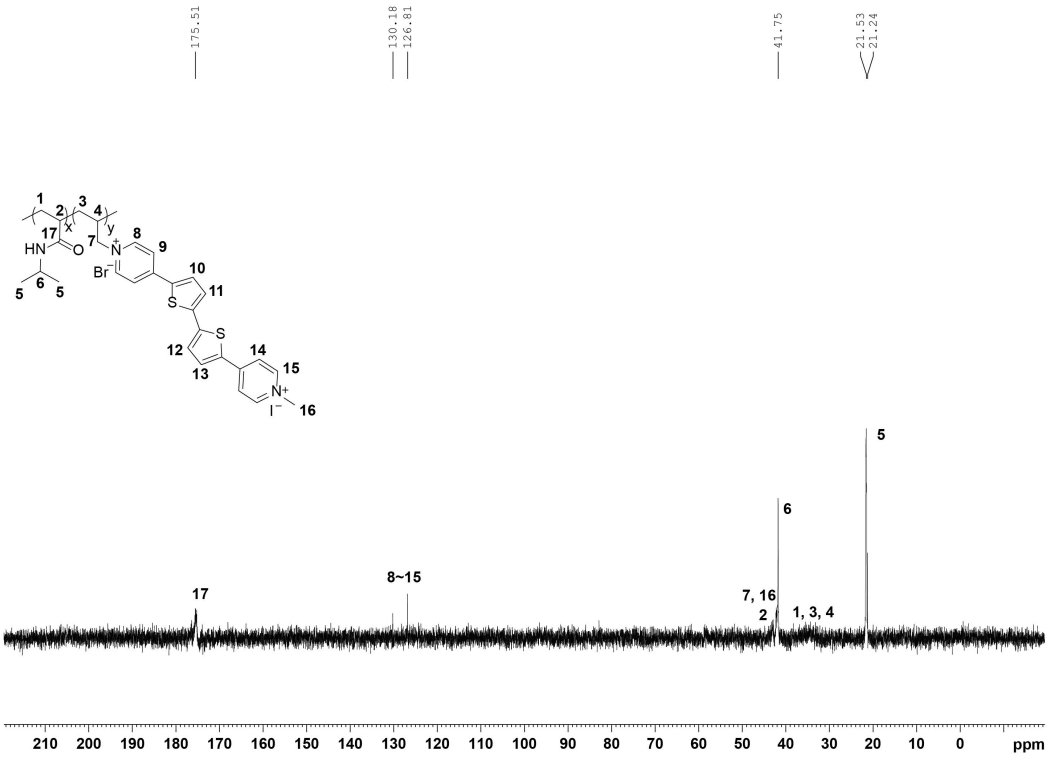

Figure S10. ^{13}C NMR spectrum for **4b** in D_2O.

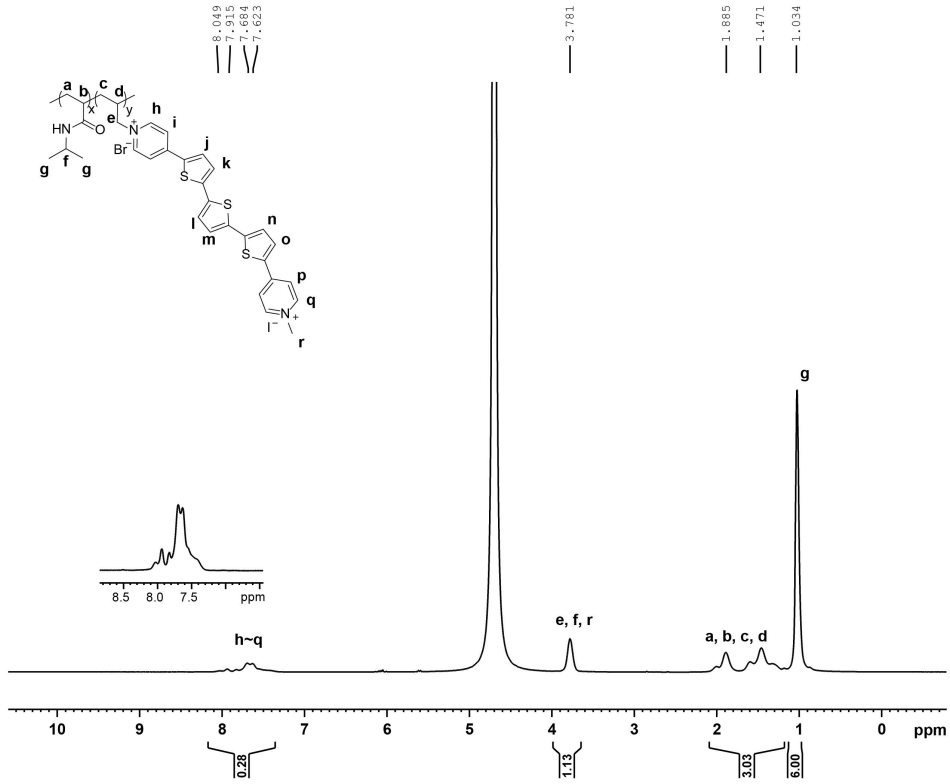

Figure S11. ^{1}H NMR spectrum for **4b** in D_2O.

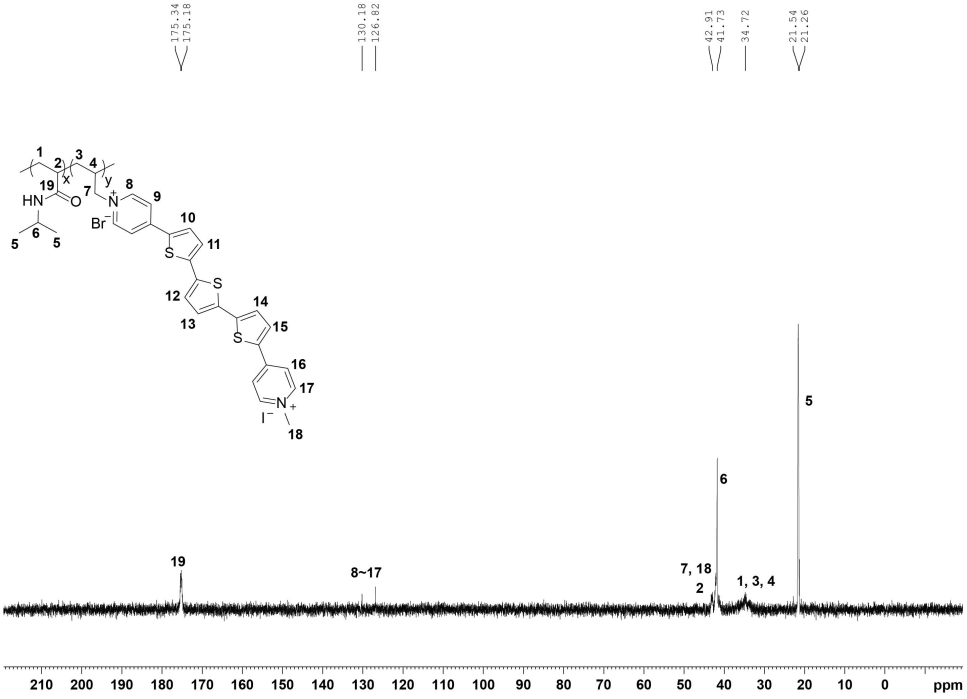

Figure S12. ^{13}C NMR spectrum for **4c** in D_2O.

4. FT-IR spectra of 4a, 4b and 4c

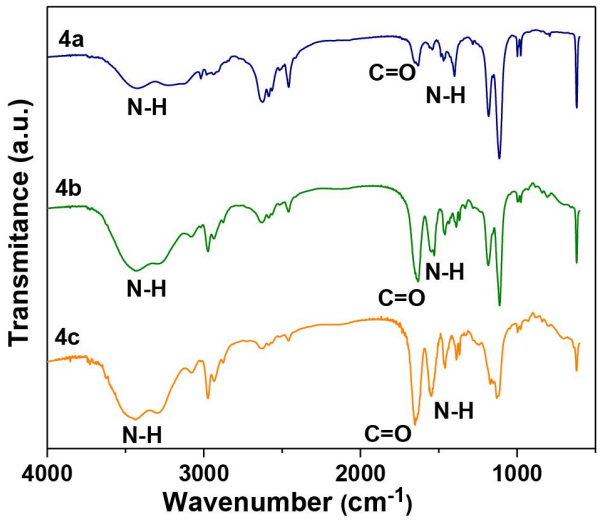

Figure S13. FT-IR spectra of **4a**, **4b** and **4c**.

5. Molecular weight analysis of 4a, 4b and 4c

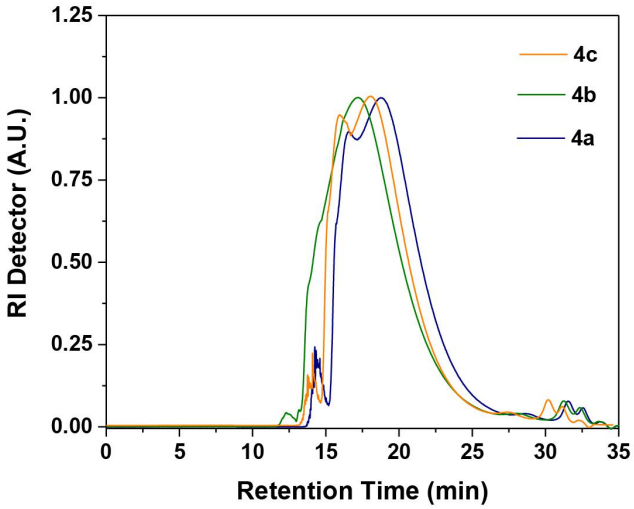

Figure S14. GPC traces of **4a**, **4b** and **4c**.

Table S1. Molecular weight analysis of **4a**, **4b** and **4c**

	M_n (g/mol)	M_w (g/mol)	M_w/M_n
4a	32600	58400	1.79
4b	39700	65300	1.64
4c	36600	61200	1.67

6. TGA and DSC analysis of 4a, 4b and 4c

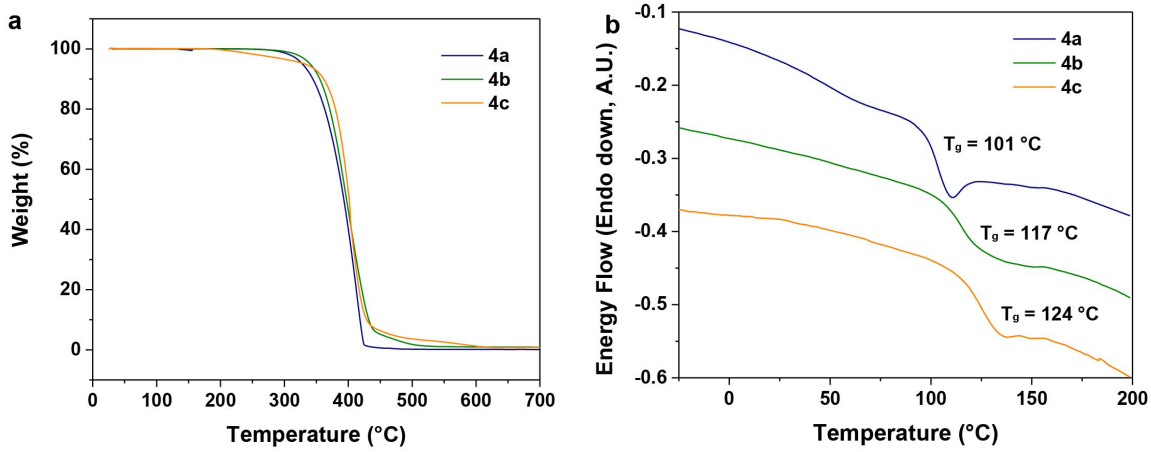

Figure S15. TGA and DSC analysis of **4a**, **4b** and **4c**

7. LCST of PNIPAM and copolymers 4a-4c

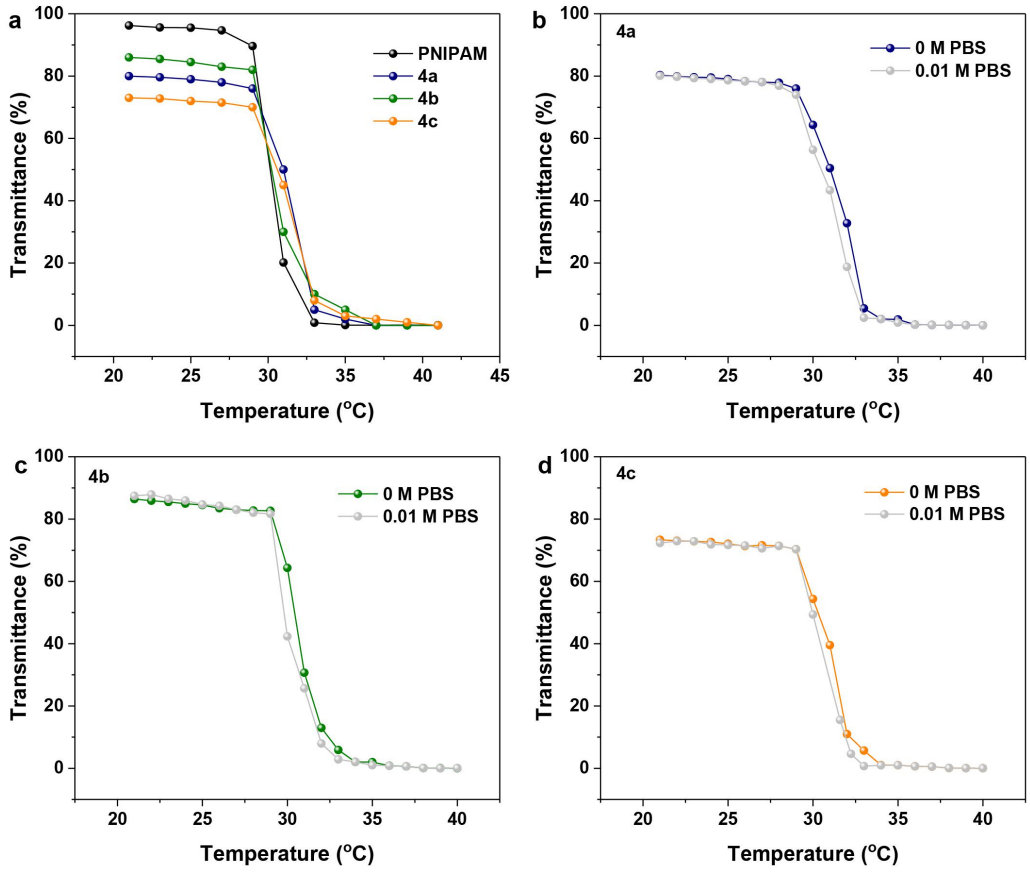

Figure S16. (a) LCST of PNIPAM and **4a-4c** in water. (b)-(d) LCST of **4a-4c** in water and 0.01 M phosphate buffer saline (PBS)

8. Cyclic voltammogram

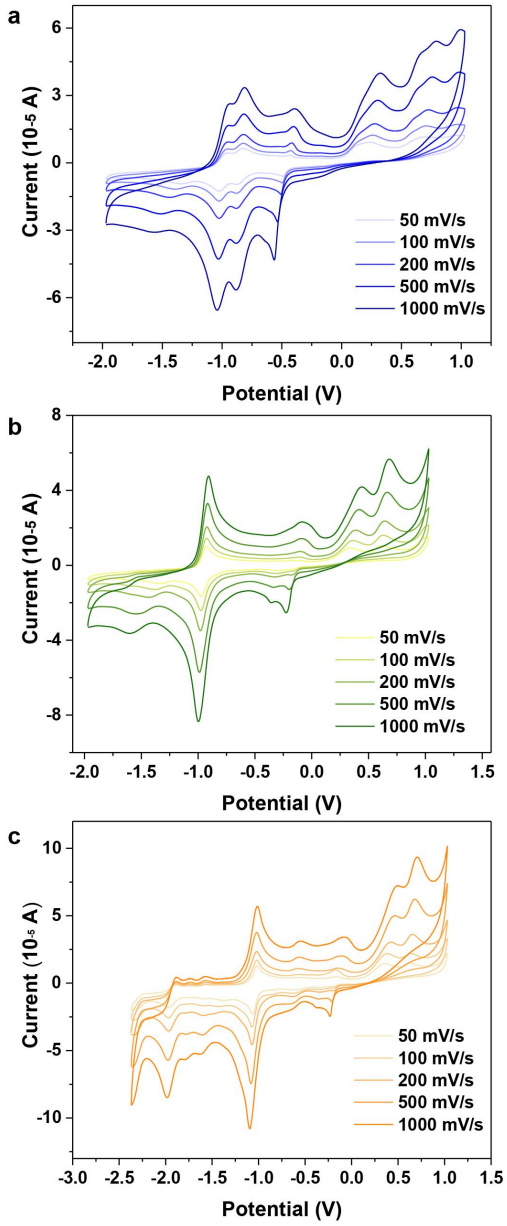

Figure S17. Cyclic voltammogram of **3a**, **3b** and **3c** (10^{-3} M in DMF solution, 0.1 M [n-Bu_4N][PF_6] as supporting electrolyte, *vs*. Fc/Fc^+)

Table S2. Electronic Properties of thienoviologen **3a**, **3b** and **3c**

	$E_{red1,1/2}$ (V)	$E_{red2,1/2}$ (V)	E_{LUMO} (eV)
3a	-0.46	-0.99	-4.23
3b	-0.92	-1.25	-3.88
3c	-1.03	-1.90	-3.77

9. Evaluation of electron-transfer constant k_{ET}

The electron-transfer constants k_{ET} were determined using the Nicholson method.[2]

$i_p = 2.69 \times 10^5 A D_0^{1/2} v^{1/2} c^* = R v^{1/2}$

where electrode radius r = 0.15 cm, electrode area $A = \pi r^2 = 0.07065$ cm^2, concentration $c^* = 10^{-6}$ mol/cm^3.

When scan rate v = 0.1 V/s,

$k_{ET} = \Psi(\frac{\pi D_0 F v}{RT})^{1/2} = 184 \Psi R$

$\Psi = (-0.6288+0.0021\Delta E_p)/(1-0.017\Delta E_p)$

Table S3. Electron-transfer constant k_{ET} of **3a**, **3b** and **3c**.

	R_1[a]	ΔE_{p1} [mV][b]	Ψ_1[c]	k_{ET1}[d]
3a	2.69×10^{-5}	72	2.13	1.05×10^{-2}
3b	2.67×10^{-5}	90	0.83	4.08×10^{-3}
3c	3.80×10^{-5}	127	0.31	2.18×10^{-3}

[a] Slope of i_p~$v^{1/2}$ in Figure S18. [b] ΔE_p was calculated from CV. [c] Ψ *was* calculated from Nicholson method for CV. [d] electron-transfer constant k_{ET} was evaluated according to Nicholson's formula.

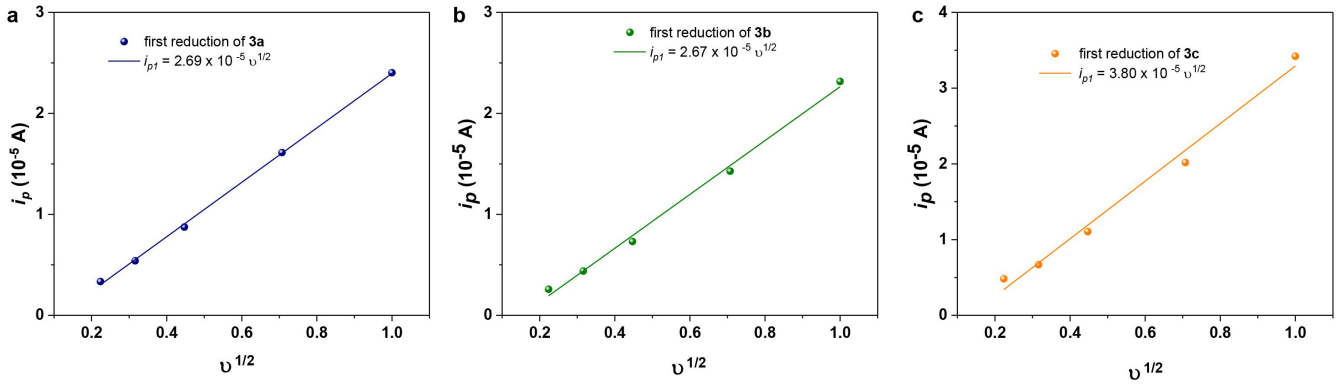

Figure S18. Peak current and scan rate diagram of **3a**-**3c**

10. UV-Vis absorption spectra at various applied voltages

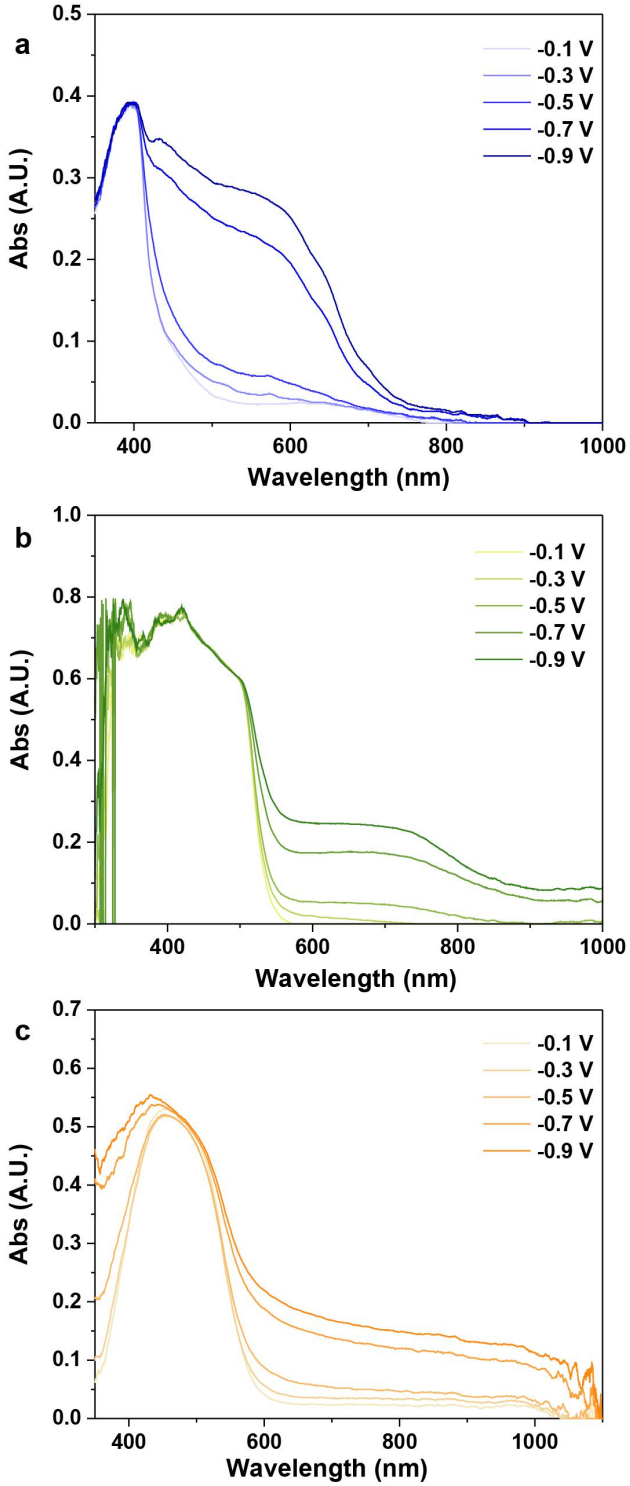

Figure S19. UV-Vis absorption of **4a-4c** at various applied voltages

11. EPR analysis of 4a-4c

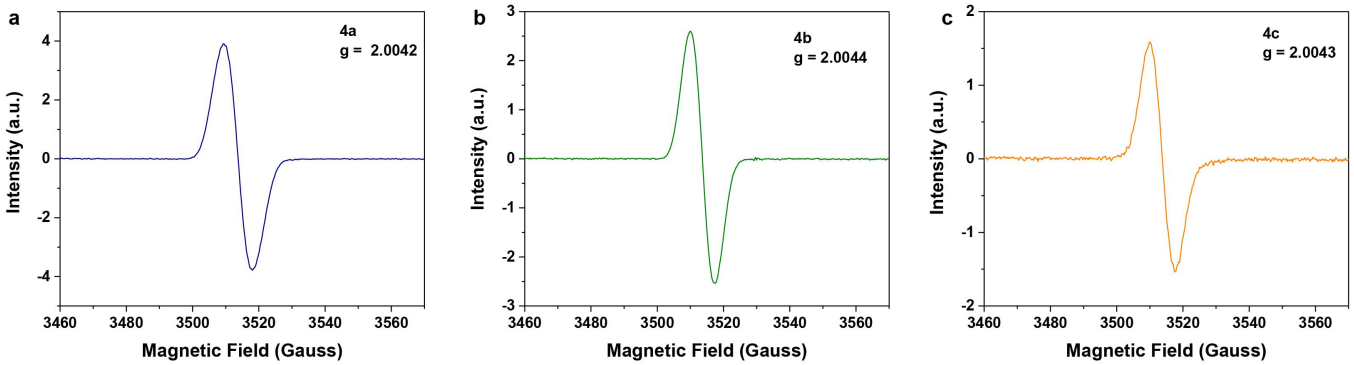

Figure S20. EPR spectra of the radical species of **4a**, **4b** and **4c**

12. Color switching behavior and coloration efficiency

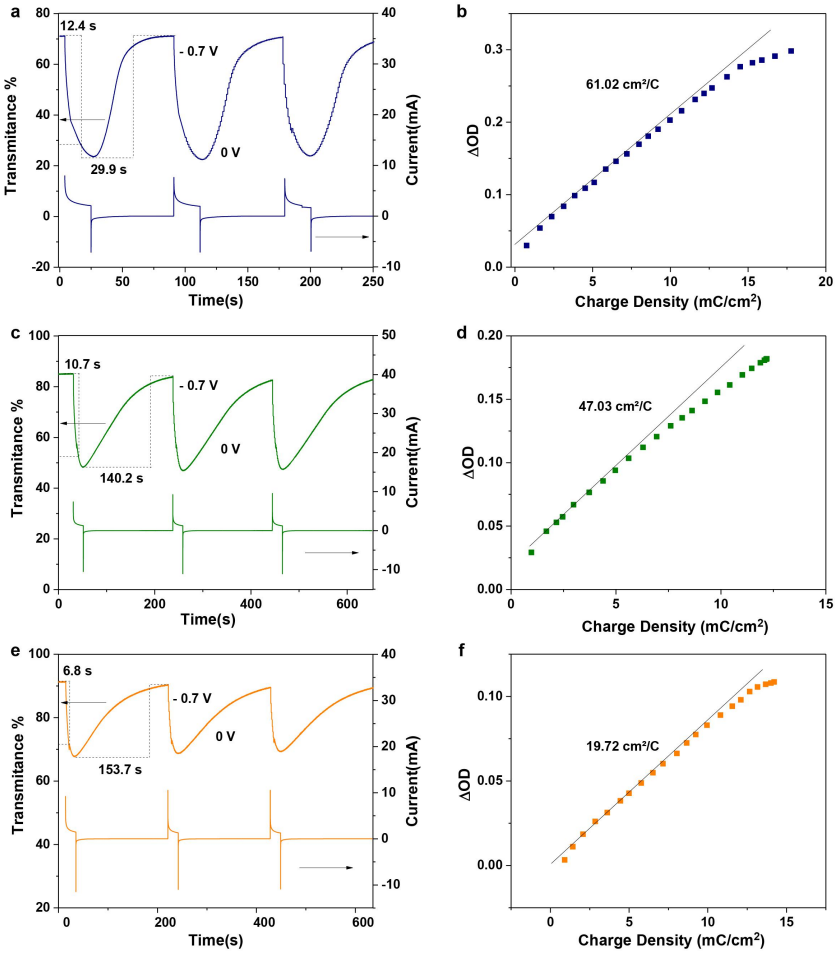

Figure S21. The color switching behavior of the ECD based on (a) **4a** (c) **4b** and (e) **4c**. The coloration efficiency of (b) **4a**, (d) **4b** and (f) **4c**

Table S4. EC switching properties of all-in-one gel ECDs containing poly(NIPAM-*co*-TV)

	λ(nm)	Optical contrast (%)	Coloration time (s)	Bleaching time (s)	Coloration efficiency ($cm^2\ C^{-1}$)
4a	560	47	12.4	29.9	61.02
4b	745	39	10.7	140.2	47.03
4c	650	25	6.8	135.7	19.72

13. UV-Vis spectra

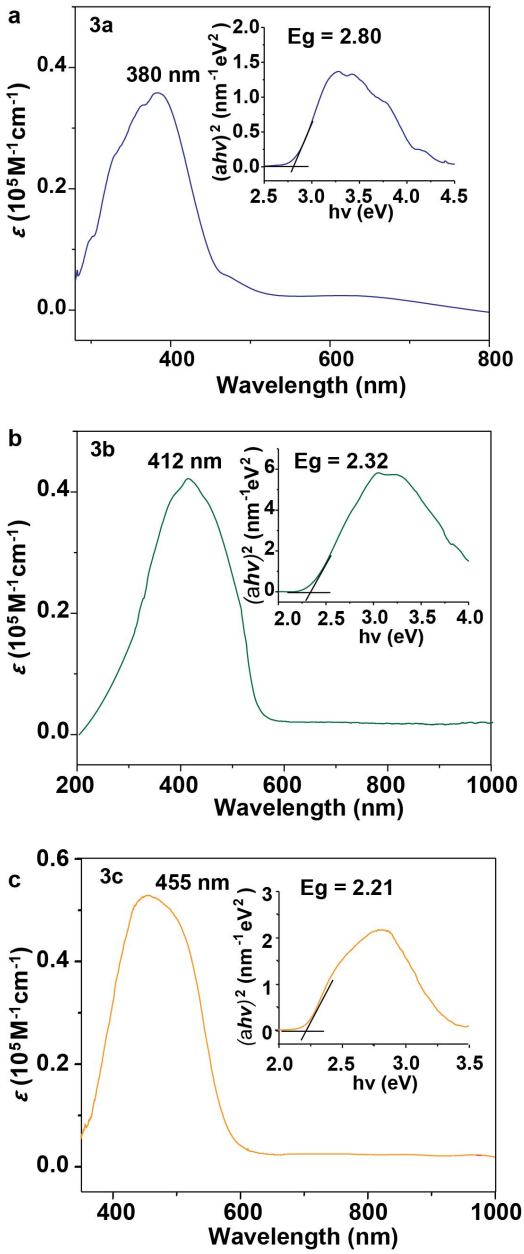

Figure S22. UV-Vis spectra of **3a**, **3b** and **3c** in H_2O.

14. Fluorescent properties

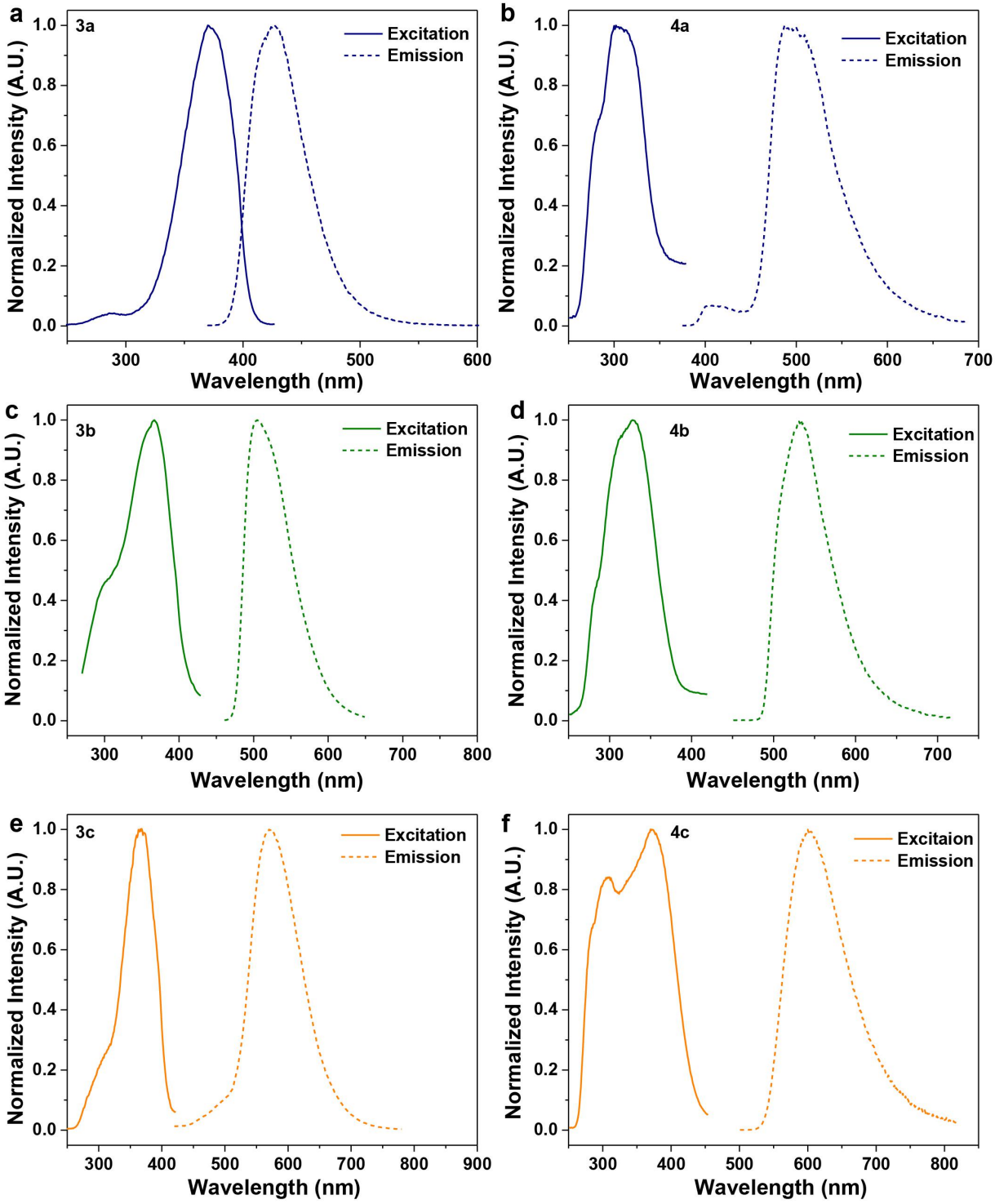

Figure S23. Fluorescent spectra of **3a-3c** and **4a-4c**

15. Zeta potential of bacteria with and without thienoviologens

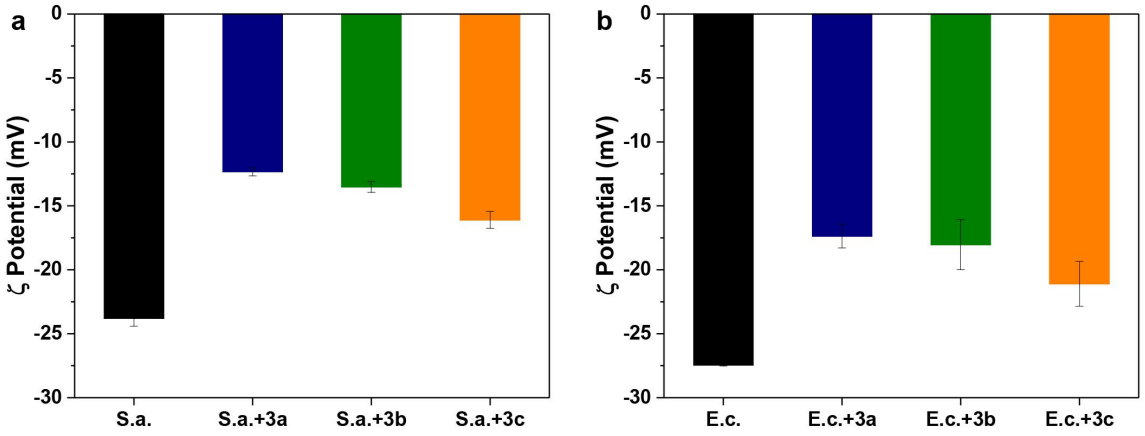

Figure S24. Zeta potential of *S. aureus* (a) and *E. coli* (b) before and after addition of **3a-3c**.

16. Bacteria encapsulation ability of 4a-4c

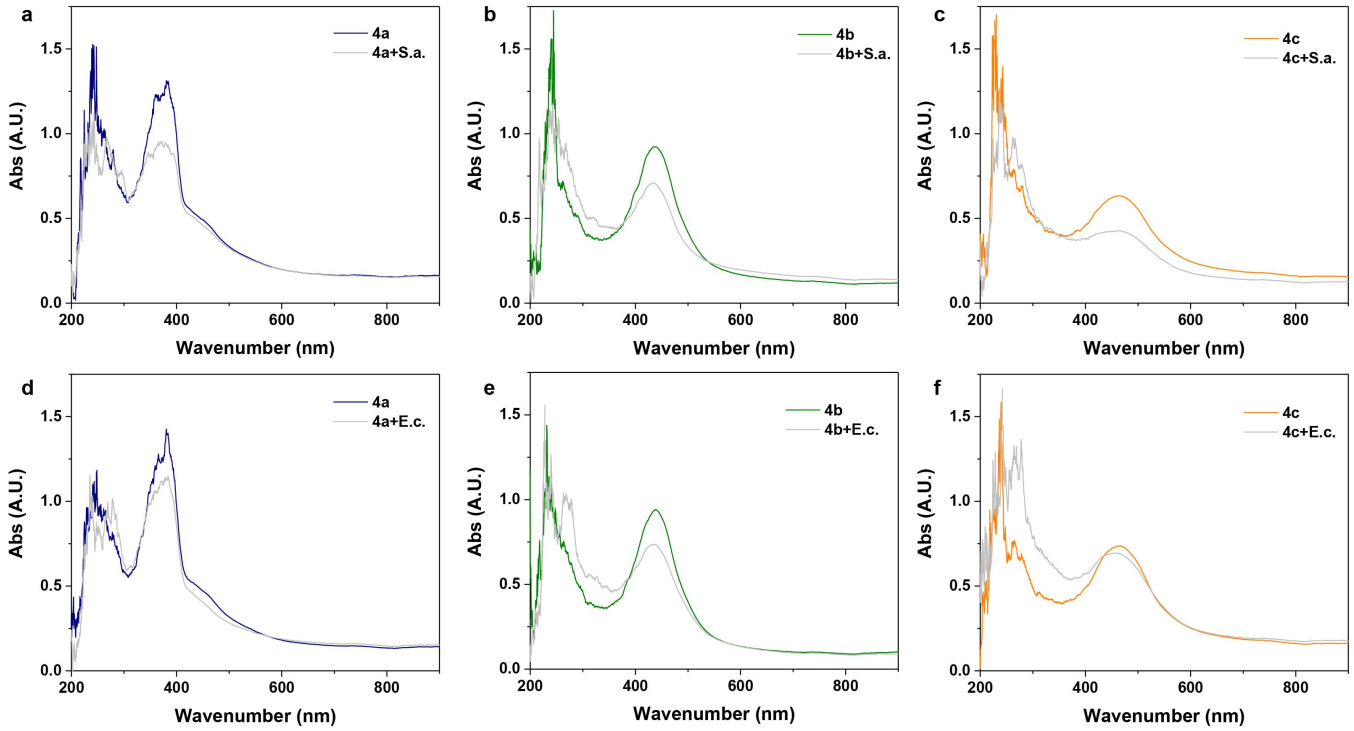

Figure S25. UV absorption spectra of **4a-4c** before and after addition of bacteria

17. Hydrophilicity of 4a-4b below and above LCST

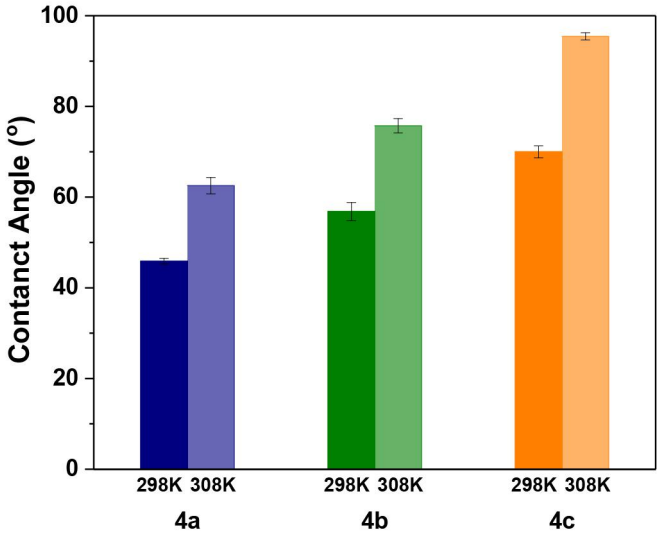

Figure S26. Water contact angle of **4a**-**4c** at 25 °C and 35 °C

18. Antibacterial activities of 4a-4c

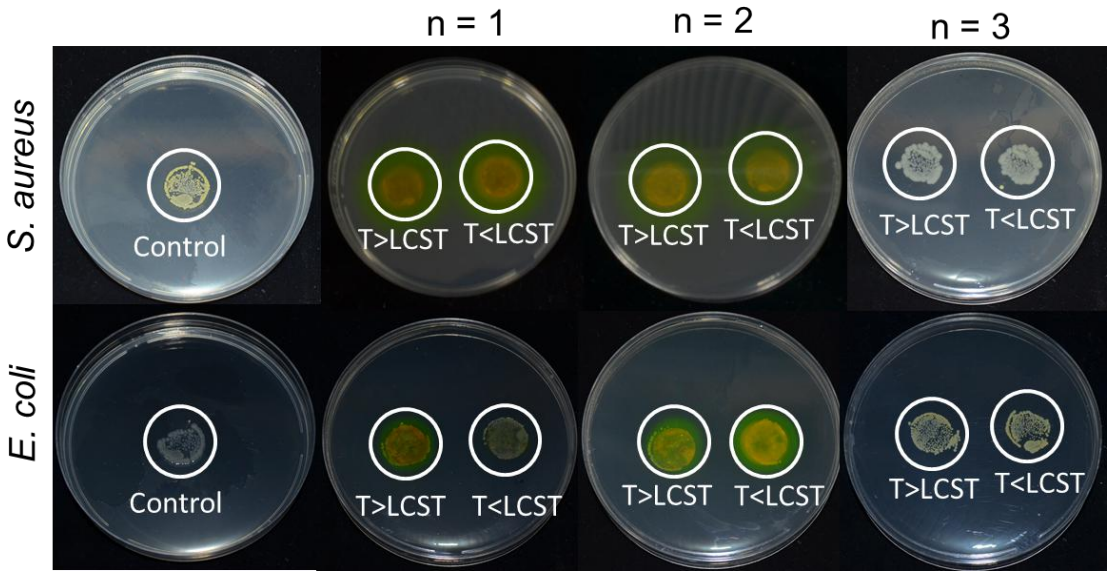

Figure S27. *S. aureus* and *E. coli* incubated with **4a**, **4b** and **4c** without irradiation

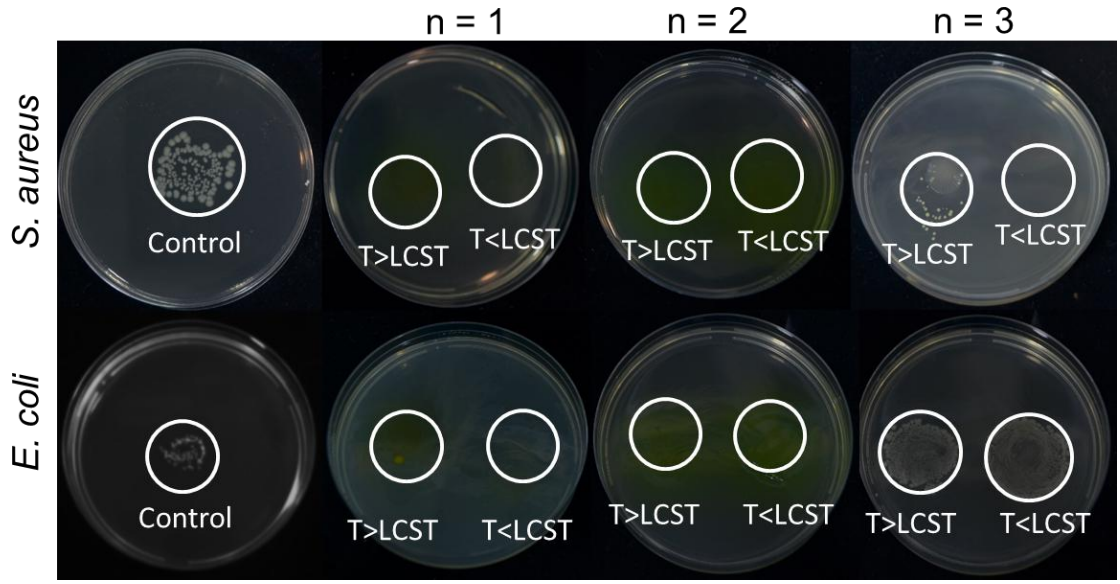

Figure S28. *S. aureus* and *E. coli* incubated with **4a**, **4b** and **4c** with white light irradiation

Supplementary References

1 E. Lim, *Mol. Cryst. Liq. Cryst.*, 2014, **602**, 251-257.

2 H. Muhammad, I. A. Tahiri, M. Muhammad, Z. Masood, M. A. Versiani, O. Khaliq, M. Latif and M. Hanif, *J. Electroanal. Chem.*, 2016, **775**, 157-162.